

Presomitic mesoderm-specific expression of the transcriptional repressor *Hes7* is controlled by E-box, T-box, and Notch signaling pathways

Received for publication, April 28, 2018, and in revised form, June 1, 2018. Published, Papers in Press, June 12, 2018, DOI 10.1074/jbc.RA118.003728

Shinichi Hayashi^{†1}, Yasukazu Nakahata^{‡2}, Kenji Kohno[§], Takaaki Matsui[‡], and Yasumasa Bessho^{‡3}

From the [†]Laboratory of Gene Regulation Research and [§]Laboratory of Molecular and Cell Genetics, Graduate School of Biological Sciences, Institute for Research Initiatives, Nara Institute of Science and Technology (NAIST), Ikoma, Nara 630-0192, Japan

Edited by Joel Gottesfeld

Somites are a pair of epithelial spheres beside a neural tube and are formed with an accurate periodicity during embryogenesis in vertebrates. It has been known that *Hes7* is one of the core clock genes for somitogenesis, and its expression domain is restricted in the presomitic mesoderm (PSM). However, the molecular mechanism of how *Hes7* transcription is regulated is not clear. Here, using transgenic mice and luciferase-based reporter assays and *in vitro* binding assays, we unravel the mechanism by which *Hes7* is expressed exclusively in the PSM. We identified a *Hes7* essential region residing -1.5 to -1.1 kb from the transcription start site of mouse *Hes7*, and this region was indispensable for PSM-specific *Hes7* expression. We also present detailed analyses of *cis*-regulatory elements within the *Hes7* essential region that directs *Hes7* expression in the PSM. *Hes7* expression in the PSM was up-regulated through the E-box, T-box, and RBPj-binding element in the *Hes7* essential region, presumably through synergistic signaling involving mesogenin1, T-box6 (Tbx6), and Notch. Furthermore, we demonstrate that Tbx18, Ripply2, and *Hes7* repress the activation of the *Hes7* essential region by the aforementioned transcription factors. Our findings reveal that a unified transcriptional regulatory network involving a *Hes7* essential region confers robust PSM-specific *Hes7* gene expression.

Establishment of cellular identities is essential for generating complex patterns during embryogenesis. To establish cellular identities and develop organ/tissue formations properly, gene expressions are spatiotemporally regulated with accuracy in appropriate domains. The *lefty1/lefty2* expressions, for example, are restricted to the left side of early developing mouse embryos to direct left–right axis determination (1). Deletion of *lefty1* or *lefty2* results in left pulmonary isomerism, malposi-

tioning of the cardiac outflow tracts, and other vascular vessels (2) or an expanded primitive streak, formation of excess mesoderm (3), and various situs defects, including left isomerism (4), respectively.

We have identified the *Hes7* gene, one of the *Hes* family transcriptional repressors, which is exclusively expressed in the presomitic mesoderm (PSM)⁴ and acts as a key molecule for somitogenesis (5–7). Somitogenesis is the process to form somites, which is a pair of epithelial spheres beside a neural tube and appear transiently during embryogenesis, from the anterior PSM (8). It is known that *Hes7* expression is restricted in the PSM and is regulated by the Notch, Fgf, and Wnt signaling pathways (9). These signaling pathways regulate various processes during embryogenesis, suggesting that the restricted *Hes7* gene expression in the PSM is orchestrated by a combination of transcriptional factors downstream of the Notch, Fgf, and Wnt signaling pathways. However, little is known about the transcriptional regulations that are associated with *Hes7* gene expression.

In this study, we describe the presence of a *Hes7* essential region, residing from -1.5 to -1.1 kb, from the transcription start site of the mouse *Hes7* gene, that directs PSM-specific *Hes7* expression. Furthermore, we demonstrate the mechanisms for *Hes7* expression in the PSM. Restricted *Hes7* expression is controlled through E-box, T-box, and the RBPj-binding element in the *Hes7* essential region, presumably activated by a synergistic effect of mesogenin1, Tbx6, and Notch signaling, and repressed by Tbx18, Ripply2, and *Hes7*. Our study uncovered that the *Hes7* essential region directs PSM-restricted expression pattern of *Hes7*, orchestrated by multiple transcriptional elements.

Results

*C region, from -1.5 to -1.1 kb upstream of TSS of mouse *Hes7*, is sufficient for accurate *Hes7* expression in the PSM*

Although *Hes7* mRNA is well known to be exclusively expressed in the PSM, the molecular mechanisms that regulate *Hes7* expression/repression remain largely unknown. To uncover molecular mechanisms of the unique *Hes7* expression in the PSM, we first tried to search for the essential region for

This work was supported by Japan Society for the Promotion of Science KAKENHI Grant JP24659086 (to Y. N.) and by Ministry of Education, Culture, Sports, Science and Technology (MEXT) KAKENHI Grant JP17H05768 (to Y. B.) and in part by The Uehara Memorial Foundation and Senri Life Science Foundation. The authors declare that they have no conflicts of interest with the contents of this article.

This article contains Figs. S1–S10 and supporting Experimental procedures.

¹ Present address: Embryology, Institute of Advanced Medical Sciences, Tokushima University, Tokushima 770-8503, Japan.

² To whom correspondence may be addressed. Tel.: 81-743-72-5472; Fax: 81-743-72-5479; E-mail: yasu-nakahata@bs.naist.jp.

³ To whom correspondence may be addressed. Tel.: 81-743-72-5470; Fax: 81-743-72-5479; E-mail: ybessho@bs.naist.jp.

⁴ The abbreviations used are: PSM, presomitic mesoderm; TSS, transcription start site; FW, forward; RV, reverse; bHLH, basic helix-loop-helix; PVDF, polyvinylidene difluoride.

Promoter elements for restricted expression of *Hes7*

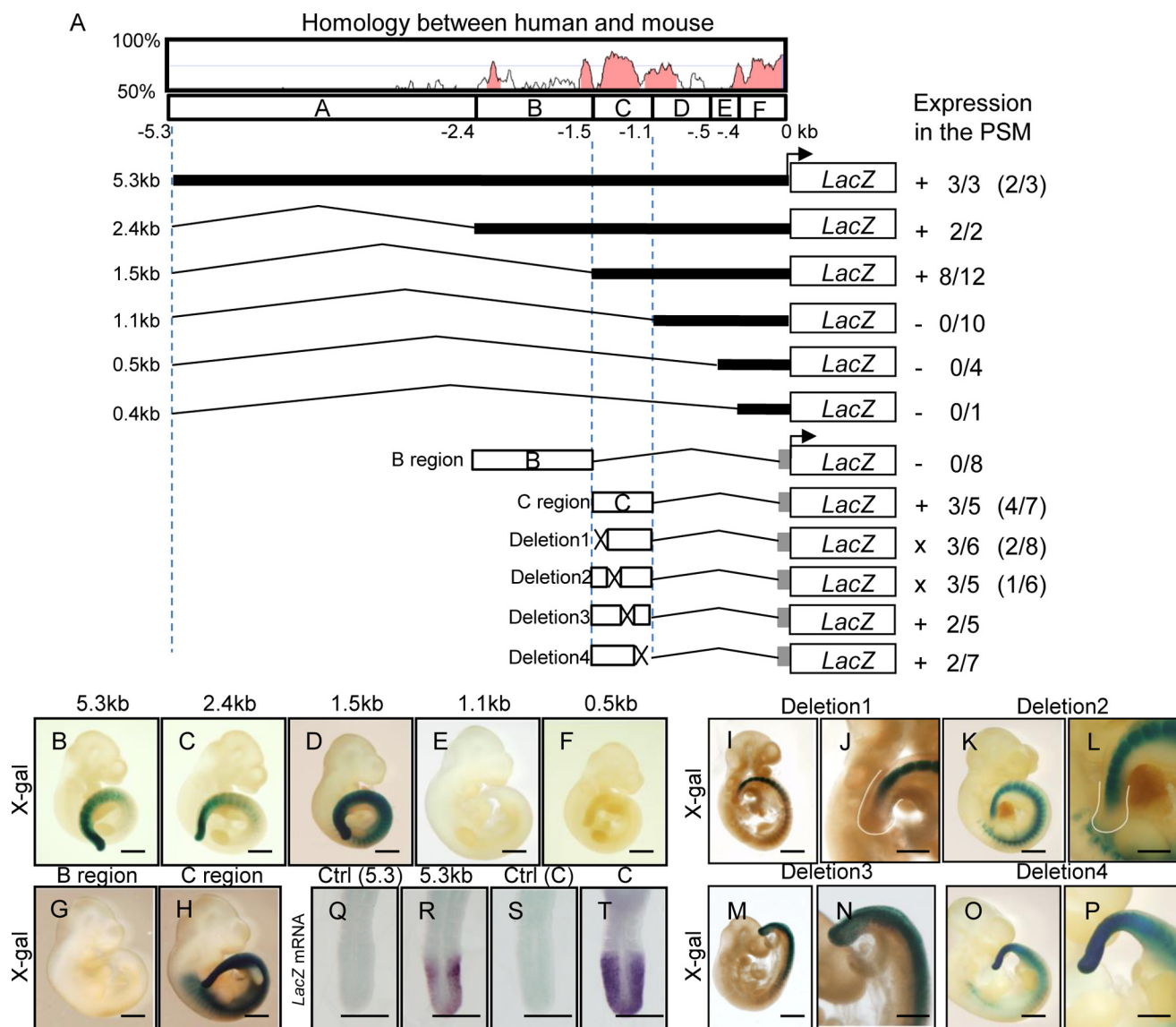


Figure 1. Regulatory elements for *Hes7* expression in the PSM. *A*, upper panel, sequence homology of *Hes7* promoter between human and mouse was shown by VISTA. Transcription start site is indicated by the arrow and set to +1. 5.3 kb of *Hes7* promoter was divided into six fragments, designated as A–F regions in this study. *A*, bottom panel, length of each reporter construct is indicated on the left. *lacZ* was used as a reporter under the control of *Hes7* promoter. β -Globin minimal promoter is shown as a gray box. Results of reporter expression in the PSM of transgenic mice are shown on the right. +, positive expression in the PSM; –, negative expression in the PSM; x, impaired expression in the PSM. Numbers indicated X-gal–positive embryos/genotyping positive embryos. Numbers in parentheses show *lacZ* mRNA–positive embryos/genotyping–positive embryos. B–F, transgenic mice integrated with the 5.3 kb (B), 2.4 kb (C), 1.5 kb (D), 1.1 kb (E), or 0.5 kb (F) of reporter were stained with X-gal at E10.5. G and H, transgenic mice integrated with the B (G) or C (H) region of *Hes7* upstream were stained with X-gal at E10.5. I–P, transgenic mice integrated Deletion1 (I and J), Deletion2 (K and L), Deletion3 (M and N), or Deletion4 (O and P) were stained with X-gal at E10.5. J, L, N, and P are magnified photos of I, K, M, and O, respectively. Q–T, transgenic embryos integrated with 5.3 kb (R), *Hes7* C region (T), or embryos that did not integrate reporter genes into genome (Q and S) were subjected to *in situ* hybridization. Scale bars, 1 mm (B–I, K, M, and O), 0.5 mm (J, L, N, and P–T).

PSM-specific *Hes7* expression by means of transgenic founder assays. All transgenic embryos ($n = 3$) carrying the 5.3-kb fragment upstream from the TSS of mouse *Hes7*, which has been utilized for exogenous *Hes7* expression in the PSM (10, 11), followed by a *lacZ* reporter showed X-gal–positive staining in the PSM at embryonic day (E) 10.5 (Fig. 1B). We next narrowed down the essential region and found that 2.4- and 1.5-kb fragments upstream from TSS were still sufficient for the reporter expression in the PSM (Fig. 1, C and D). However, we could not detect any X-gal–positive staining in the PSM of transgenic mice carrying a 1.1-kb fragment or shorter fragment (Fig. 1, E and F). These results suggest that the 1.5-kb fragment is suffi-

cient for the PSM-specific expression of *Hes7* and that the essential region for PSM-restricted expression of *Hes7* resides between –1.5 and –1.1 kb upstream of TSS.

To confirm the region responsible for PSM-specific expression of *Hes7*, we next investigated the fragment from –2.4 to –1.5 kb, which is not considered to be an essential region for PSM-specific *Hes7* expression, and hereafter it is referred to as the B region; and the fragment from –1.5 to –1.1 kb is hereafter referred to as the C region (Fig. 1A). Transgenic founder assays revealed that the C region drove β -gal protein expression in the PSM, whereas the B region had no β -gal activity in the PSM (Fig. 1, G and H). Next, we narrowed down the essential

region in the C region. We constructed four reporter vectors deleting a quarter of fragment C region named Deletion1, -2, -3, or -4 (Fig. 1A and Fig. S1). Deletion1 and -2 showed no X-gal-positive staining at the most posterior end of the PSM (Fig. 1, I–L). However, Deletion3 and -4 resulted in X-gal-positive staining comparable with the WT C region (Fig. 1, M–P). *In situ* hybridization also demonstrated that the anterior-most regions of the PSM were negative for Deletion1- and -2-driven *lacZ* mRNA (Fig. S2). We therefore deduce from the above results that the 0.4-kb C region is the essential region, and the distal half of the C region from TSS contains essential transcriptional binding sites for *Hes7* expression in the PSM.

Although endogenous *Hes7* mRNA was expressed exclusively in the PSM, X-gal-positive staining was present throughout the PSM and newly formed somites, which are derived from the PSM, in transgenic mice carrying 5.3-, 2.4-, 1.5-kb fragments or the C region (Fig. 1, B–D and H). A simple explanation was that the reporter mRNA was transcribed exclusively in PSM cells, whereas its resultant β -gal protein remained in differentiated somite cells due to high protein stability. To assess this possibility, we carried out *lacZ* mRNA detection by *in situ* hybridization. The *lacZ* mRNA driven by a 5.3-kb fragment or the C region was exclusively expressed in the PSM (Fig. 1, R and T), and as expected, the control mice without transgene did not show any signal in the PSM (Fig. 1, Q and S). These results demonstrate that the C region is sufficient for accurate *Hes7* expression in the PSM.

E-boxes in C region are essential to drive *Hes7* in the PSM

To address which transcriptional binding elements regulate PSM-specific *Hes7* expression, we searched for putative transcriptional binding elements within the C region by *in silico* analyses. There are several putative regulatory sequences in the C region: three T-boxes (YMACACYY or complementary) (21); six E-boxes (CANNTG) (5); and one RBPj-binding site (YRTGDGAD or complementary) (Fig. 2A and Fig. S1) (37), in particular, E-box1, -3, -5, and -6 and T-box2 were completely conserved among *Homo sapiens*, *Pongo abelii*, *Bos taurus*, and *Mus musculus* (Fig. 2A). To address whether these putative E-boxes, T-boxes, and the RBPj-binding site in the C region are functional *in vivo*, we made transgenic mice carrying the mutated E-box1–6/C region or the mutated T-box1 and -2/C region, which also include a mutated RBPj-binding site. *In situ* hybridization assays using transgenic founder mice revealed that mice with the mutated T-box1 and -2/C region expressed the reporter mRNA in the PSM as well as the mice with WT C region (Fig. 2B, panels a and b). In contrast, 14 of 16 mice with the mutated E-box1–6/C region showed no positive signal, whereas only two embryos showed a dispersed and straggling reporter expression (Fig. 2B, panels c and d, and Fig. S3), indicating that E-boxes in the C region are essential to drive *Hes7* in the PSM.

Msgn1, *Tbx6*, and Notch signaling pathway activate C region *in vitro*

To investigate the putative elements in the C region in depth, we performed luciferase assays using constructs containing the WT or mutated C region followed by a human β -globin mini-

mal promoter. To perform this, mesogenin1 (*Msgn1*), *Tbx6*, and NICD, the intracellular domain of Notch1, were utilized as binding factors for E-box, T-box, and RBPj-binding site, respectively. This is based on previous reports that showed that *Msgn1*, a bHLH-type transcription factor, is exclusively expressed in the posterior PSM (12), whereas *Tbx6*, a T-box family of transcriptional factor, and Notch signaling molecules are expressed ubiquitously in mouse PSM (13–15). We confirmed that the *Msgn1* expression domain coincided with *Hes7* stripes in phase I and II, but not at phase III, whereas *Tbx6* mRNA was constantly distributed over the PSM, overlying any phases of the *Hes7*-transcribed region, besides the anterior-most region of the PSM (Fig. S4). WT C region reporter was activated by all of the transcriptional factors tested (Fig. 3, A–C), whereas the activity of mutated E-box1–6/C or T-box1–3/C region reporter was attenuated by *Msgn1* or NICD, respectively, (Fig. 3, A and B), indicating that at least one of the mutated E-boxes is a functional site for *Msgn1*, whereas the T-box1 is receptive toward Notch signaling molecules. However, the mutated T-box1–3/C region reporter was still responsive to *Tbx6*, comparable with that of WT C region (Fig. 3C).

To further investigate E-boxes, T-boxes, and the RBPj-binding site in the C region *in vitro*, we performed oligo-DNA pull-down assay and electrophoretic mobility shift assay (EMSA). Pull-down assay revealed that *Msgn1* bound to E-box1, but not to E-box2 and -3 (Fig. 3D). Furthermore, we confirmed that *Msgn1* binding to the E-box1 was abolished by the mutation of E-box1 (Fig. 3D). EMSA also demonstrated that *Msgn1* bound to E-box1, but not to E-box2 and -3 (Fig. S5). Again, we confirmed that *Msgn1* binding to E-box1 was abolished by an excess amount of the nonlabeled E-box1 but not by that of the mutant one (Fig. S5). These results raise the possibility that *Msgn1* in the PSM activates *Hes7* expression via the E-box1 in C region. RBPjk binding was detected by T-box1, in which RBPj-binding site is included, by pull-down assay and EMSA (Fig. 3E and Fig. S6). Moreover, pull-down assay demonstrated that RBPjk binding was dramatically attenuated by the mutated E-box1, and EMSA showed that this binding was attenuated by an excess amount of the nonlabeled E-box1 but not by that of the mutated one (Fig. 3E and Fig. S6). These results raise the possibility that the RBPj-binding site in C region is functional *in vivo*. Luciferase assays demonstrated that T-box1–3 were not responsive to *Tbx6*; however, ChIP assay utilizing PSM samples indicated that *Tbx6* bound to the C region (Fig. S7A). To investigate whether *Tbx6* binds to T-box elements in the C region, we performed oligo-DNA pull-down assay and showed that *Tbx6* bound to T-box1 and T-box2 but not to T-box3. In contrast, the *Tbx6* binding potential to T-box1 or T-box 2 was eliminated by mutated T-box1 or T-box2, respectively (Fig. S7 and data not shown).

Msgn1, *Tbx6*, and Notch signaling pathways synergistically activate C region *in vitro*

As we demonstrated that *Msgn1* and NICD increased the luciferase activity of the C region and *Msgn1* and RBPjk bound to E-box1 and T-box1, respectively (Fig. 3, A–E), we next investigated whether a combination of *Msgn1* and NICD show a coordinated activation. Compared with single *Msgn1* or NICD

Promoter elements for restricted expression of *Hes7*

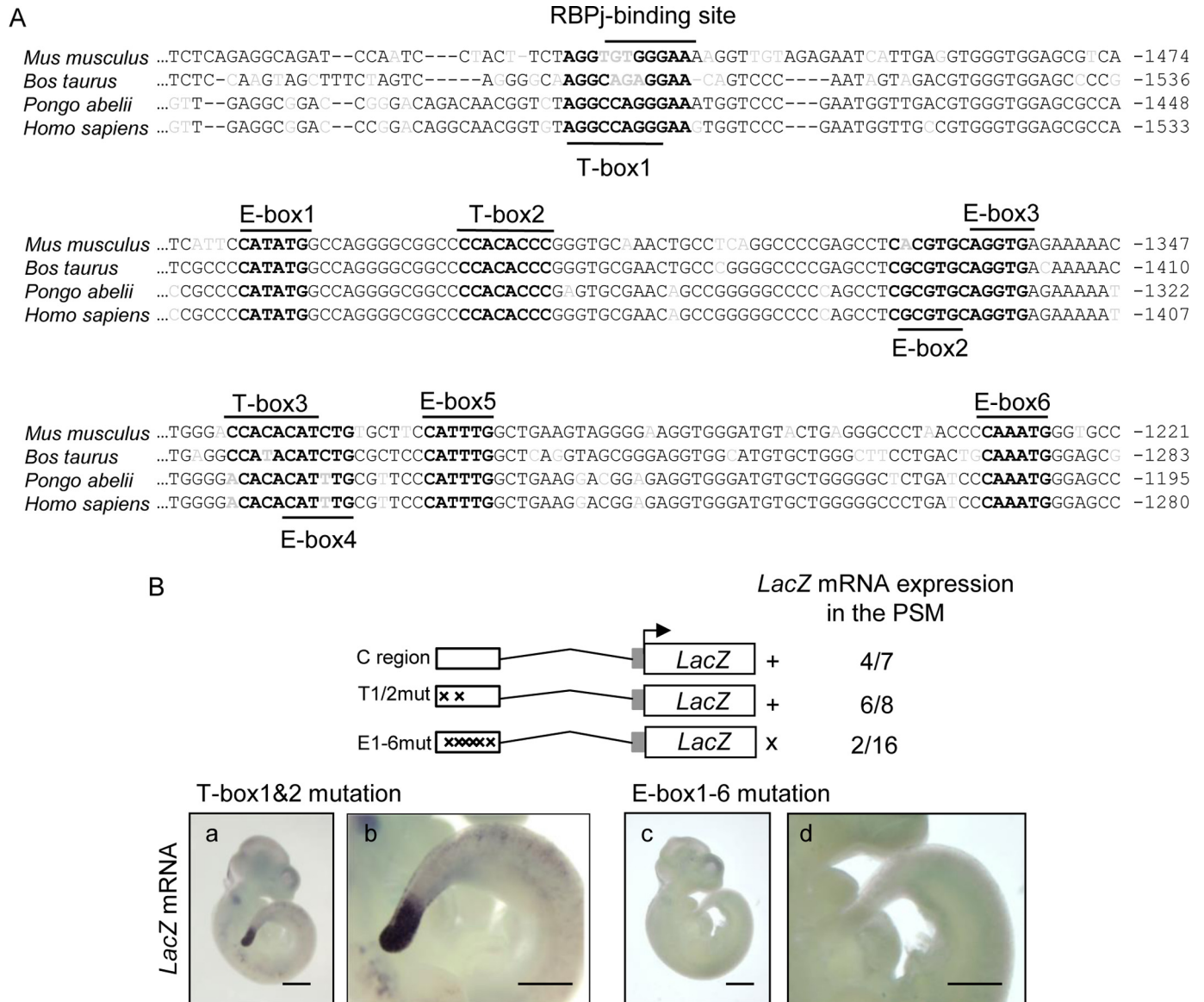


Figure 2. E-boxes in the C region are necessary for *Hes7* expression in the PSM. A, putative T-boxes (YMACACY or complementary) (21), E-boxes (CANNTG) (5), and the RBPj-binding site (YRTGDGAD or complementary) (37) within the *Hes7* C region are shown in **bold**. One base mismatch is allowed for T-box and RBPj-binding site sequences. Nonconserved sequences among species are shown in *gray*. Numbers on the right indicate the positions from transcriptional start sites. B, *in situ* hybridization of transgenic mice embryos carrying *lacZ* reporter under the control of Tbox1 and -2 mutant (panels a and b) or E-box1–6 mutant (panels c and d) at E10.5 were performed. β -Globin minimal promoter is shown as a gray box. Transcription start site is indicated by the arrow. Results of *lacZ* expression in the PSM of transgenic mice are shown on the right. +, positive expression in the PSM; x, impaired expression in the PSM. Numbers on the reporter constructs showed *lacZ* mRNA-positive embryos/genotyping positive embryos. Panels b and d are magnified photos of panels a and c, respectively. Scale bars, 1 mm (panels a and c), 0.5 mm (panels b and d).

activation, co-expression of *Msgn1* and *NICD* synergistically increased luciferase activity (Fig. 3F). Although, as shown above, T-box1 and -2 were not necessary for the expression of *Hes7* in the PSM (Fig. 2B, panels a and b), the ChIP assay, oligo-DNA pulldown assay, and luciferase assay showed that Tbx6 could bind to and activate the C region (Fig. 3C and Fig. S7). Furthermore, because Tbx6 has been known to work synergistically with other transcriptional activators for gene expressions in the PSM (13), we investigated the possibility of Tbx6 working synergistically with *Msgn1* or *NICD* to activate the C region. In contrast to either *Msgn1* or *NICD* alone, the combination of Tbx6 with either *Msgn1* or *NICD* increased the C region-driven luciferase activity (Fig. 3G). Intriguingly, we

revealed that Tbx6 together with *Msgn1* and *NICD* accelerated the reporter expression much more than the combinations with Tbx6/*Msgn1*, Tbx6/*NICD*, or *Msgn1*/*NICD* (Fig. 3G). These results indicate that Tbx6, *Msgn1*, and Notch signaling activate *Hes7* expression coordinately via the C region at least *in vitro*. To confirm whether their synergistic effect on the C region is due to E-boxes, T-boxes, and the RBPj-binding site, we next performed luciferase assays using the C region with the mutated T-box1–3/or E-box1–6/C region. Synergistic activation by *Msgn1*/*NICD*/Tbx6 was almost completely abolished in T-box or E-box mutants (Fig. 3H), although activity in the T-box1–3 mutant was higher than that of the E-box1–6 mutant, supporting the results that embryos with mutated

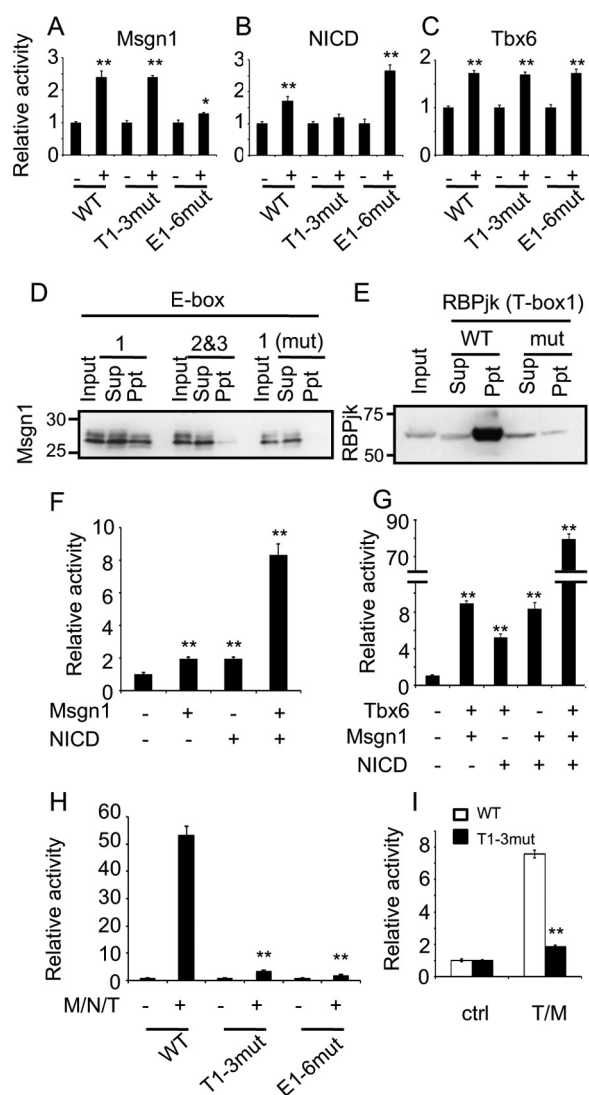


Figure 3. Msgn1, Tbx6, and Notch signaling act on *Hes7* expression. A–C, luciferase assays for wildtype (WT), T-box mutant (T1–3mut), or E-box mutant (E1–6mut) *Hes7* C region with or without Msgn1 (A), NICD (B), or Tbx6 (C) were performed in NIH3T3 cells. Reporter firefly luciferase activities were normalized by *Renilla* luciferase activities under SV40 promoter. Data represent the means \pm S.E. of three independent samples. D, oligo-DNA pull-down assays against Ebox1 (WT/mut) or E-box2/3 (WT) with Msgn1-Myc were performed. Sup, supernatant; Ppt, Msgn1 was revealed with anti-Myc. E, oligo-DNA pull-down assays against T-box1 (WT/mut) with RBPjk-Myc were performed. RBPjk was revealed with anti-Myc. Sup, supernatant; Ppt, precipitate. F–I, luciferase assays for WT (F and G) or indicated mutant (H and I) *Hes7* C region with indicated transcription factors were performed. Reporter firefly luciferase activities were normalized by *Renilla* luciferase activities under SV40 promoter. Data represent the means \pm S.E. of three independent samples. *, $p < 0.05$; **, $p < 0.01$ compared with no transcription factor control for each promoter (A–C, F, and G), Msgn1 (M)/NICD (N)/Tbx6 (T) for WT promoter (H) or Tbx/Msgn1 for WT promoter (I) (Student’s two-tailed *t* test).

T-box1 and -2 expressed *lacZ* mRNA, but those with E-box1–6 did not, *in vivo* (Fig. 2B). We further investigated whether the participation of Tbx6 in the synergistic activation is independent of T-box1–3 elements. To address that, we evaluated the synergistic effect of Tbx6 and Msgn1 to rule out the activation of T-box1 by NICD. Surprisingly, the activation of the mutated T-box1–3/C region by Tbx6 and Msgn1 was almost completely abrogated (Fig. 3J), suggesting that T-box1–3 elements are important for the synergistic effect of Msgn1/NICD/Tbx6 on

Hes7 expression, although T-box1–3 elements were not necessary for the single activation by Tbx6 (Fig. 3C). In contrast, the activation of the C region with E-box1–6 mutant by Tbx6 and Msgn1 was completely abolished (Fig. S8), which was similar to the result by Msgn1/NICD/Tbx6 (Fig. 3H), indicating that E-boxes are essential for the synergistic *Hes7* expression. Taking these *in vitro* and *in vivo* results together (Figs. 2 and 3), we deduce that E-boxes and T-boxes, including the RBPj-binding site, are critical and auxiliary for *Hes7* expression, respectively.

Tbx18, Ripply2, and Hes7* repress the activation of C region *in vitro

Transgenic mice carrying the mutated T-box1 and -2/C region or Deletion1 expressed *lacZ* mRNA not only in the PSM but also expressed a dispersed and straggling reporter mRNA in the somites (Fig. 2B, panel b, and Fig. S2), suggesting that the C region, especially T-boxes, has a role in preventing ectopic *Hes7* expression. To understand the molecular mechanisms of how *Hes7* expression in the anterior-most PSM or in somites is suppressed, we next investigated the repression mechanisms for *Hes7*. *Tbx18* is one of the transcriptional repressors among the T-box family of transcriptional factor genes that is expressed in mouse PSM (13), and as reported previously (16), *Tbx18* is expressed in the rostral part of somites and the anterior-most PSM where *Hes7* propagation has vanished (Fig. S4, C and C’), demonstrating that *Tbx18* and *Hes7* expressions are mutually exclusive. We investigated whether Tbx18 binds to T-boxes in the C region by oligo-DNA pull-down assay and EMSA. The pull-down assays demonstrated that Tbx18 bound to WT T-box1 but not to T-box2 or -3 (Fig. 4A and Fig. S9A). Tbx18 binding to T-box1 was diminished by the mutation of T-box1 (Fig. 4A). EMSA also showed that Tbx18 bound to T-box1 but not to T-box2 or -3 (Fig. S9B). Again, we demonstrated that Tbx18 binding to T-box1 was weakened by an excess amount of the nonlabeled T-box1 but not by that of the mutated one (Fig. S9B). Furthermore, luciferase assays revealed that Tbx18 dose-dependently repressed reporter activity induced by Tbx6 and NICD (Fig. 4B), which are expressed at the anterior-most PSM (Fig. 5 and Fig. S4).

Ripply2 mRNA was strongly expressed, as reported previously (17), in the anterior PSM (prospective somites S0 and S-1) when *Hes7* was in phase I (Fig. S4D), whereas in phase III of *Hes7*, *Ripply2* showed two weak stripes at the region where *Hes7* is lost (Fig. S4D’). Because Ripply co-repressors have been known to act on the repressor by interacting with *Xenopus* Tbx6 or zebrafish Tbx24, which are structurally related to mouse Tbx6 (18, 19), we performed co-immunoprecipitation assays in culture cells, HEK293T, to examine whether mouse Ripply co-repressors interact with mouse Tbx6. We revealed that Ripply1/2 form a complex with Tbx6 *in vitro* (Fig. 4C), especially Ripply2, which had a high affinity to Tbx6. Luciferase assay further uncovered that luciferase activities of the C region induced by Tbx6/NICD were reduced by Ripply2 (Fig. 4B). Moreover, co-expression of Tbx18 and Ripply2 repressed luciferase activity more effectively compared to when either Tbx18 or Ripply2 was expressed, suggesting that Tbx18 and Ripply2 repress the C region independently. These results raise the pos-

Promoter elements for restricted expression of *Hes7*

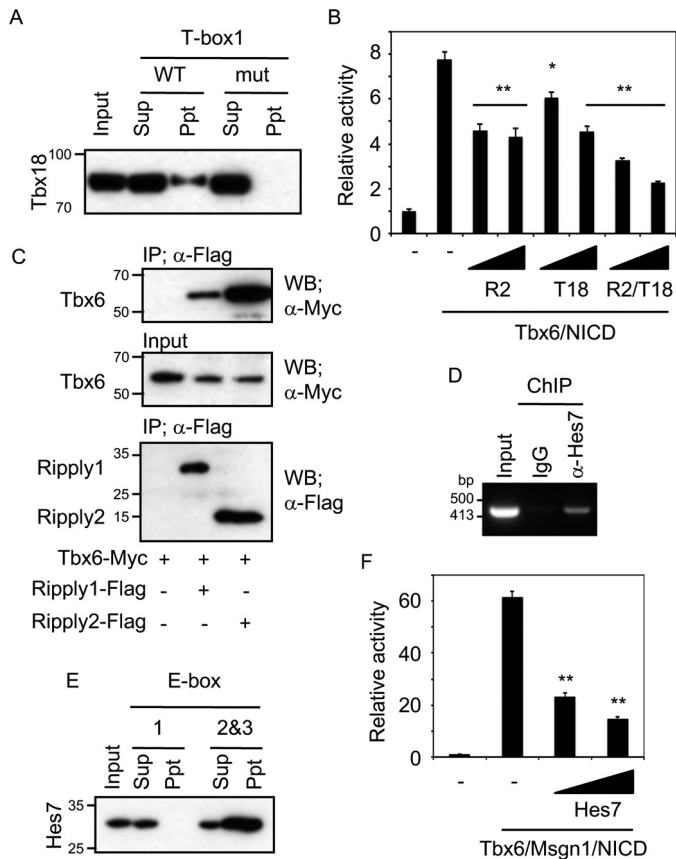


Figure 4. Transcription repressors regulate *Hes7* expression. *A*, oligo-DNA pull-down assays against WT or mutant T-box with Tbx18-FLAG were performed. Tbx18 was revealed with anti-FLAG. *B*, luciferase assay for *Hes7* C region reporter with indicated repressors in NIH3T3 cells. 100 or 200 ng of expression vectors of Ripply2 (R2) and/or Tbx18 (T18) were co-transfected with Tbx6 and NICD. Data represent the means \pm S.E. of three independent samples. *C*, co-immunoprecipitation assays were performed with Ripply1-FLAG or Ripply2-FLAG and Tbx6-Myc in HEK293T cells. Tbx6 and Ripply1/2 were revealed with anti-Myc and anti-FLAG, respectively. *D*, ChIP assays with anti-Hes7 antibody or normal rabbit IgG (negative control) were performed using mouse PSM. Resultant genomic fragment was amplified using *Hes7* C region-specific primer. *E*, oligo-DNA pull-down assays against E-box1 or E-box2 and -3 with FLAG-Hes7 were performed. Hes7 was revealed with anti-FLAG. *F*, luciferase assay for *Hes7* C region reporter with Hes7 in NIH3T3 cells. 100 or 200 ng of expression vectors of Hes7 were co-transfected with Tbx6, Msn1, and NICD. *, $p < 0.05$; **, $p < 0.01$ compared with Tbx6/NICD without repressors (*B*) or Tbx6/Msn1/NICD without Hes7 (*F*) (Student's two-tailed *t* test). *Sup*, supernatant; *Ppt*, precipitate; *WB*, Western blotting; *IP*, immunoprecipitation.

sibility that Tbx18 and Ripply2 are repressive regulators for *Hes7* termination in the anterior-most PSM and somites by binding to T-box1 or by forming a complex with Tbx6 to reduce Tbx6 transcriptional activity, respectively.

Because Hes7 could bind to the E-box to repress transcriptional activity (5), we investigated whether E-boxes in the C region are functional for *Hes7*. We first demonstrated that Hes7 binding to the C region *in vivo* was detected by ChIP assay using mouse PSM (Fig. 4D). Furthermore, the oligo-DNA pull-down assay showed that Hes7 could bind to E-box2 and -3 but not to E-box1 (Fig. 4E). Moreover, luciferase assays demonstrated that Hes7 repressed synergistic Msn1/Tbx6/NICD activation dose-dependently (Fig. 4F). These results suggest that the C region might also be associated with the oscillatory expression of *Hes7*.

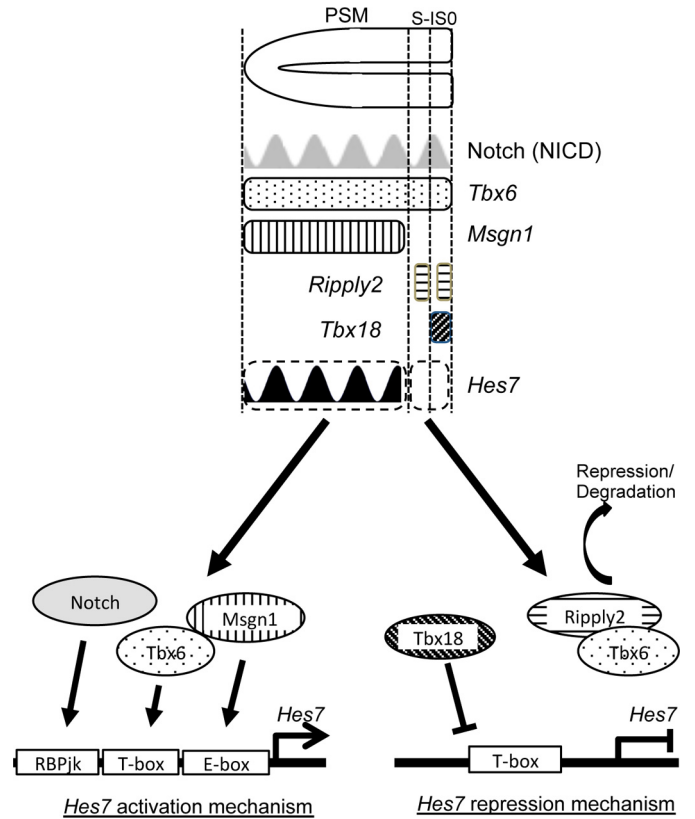


Figure 5. Scheme for restricted *Hes7* expression in the PSM. See Fig. S2 for expression domains of *Tbx6*, *Msn1*, *Ripply2*, and *Tbx18*. In the PSM (except anterior-most region), constant expressions of *Tbx6* and *Msn1* and rhythmic expression of Notch activate *Hes7* expression, and at the anterior-most region (S-1 and S0), loss of *Msn1* expression and appearance of *Ripply2* and *Tbx18* expressions suppressed *Hes7* expression.

DNA methylation is not correlated with the mechanism for the PSM-specific expression of *Hes7*

Finally, we sought to investigate whether epigenetic regulations, especially DNA methylation, of the C region take part in the repression of *Hes7* ectopic expression. To that end, we examined the DNA methylation status of the C region by bisulfite sequencing. However, no CpG sites within the C region were methylated in all the tissues tested, including PSM, head, and caudal trunk from E10.5 embryo (Fig. S10). Experimental procedures for this bisulfite sequence are provided in the supporting Experimental procedures. This result suggests that the regulation by DNA methylation is not correlated with the mechanism for the PSM-specific expression of *Hes7*.

Discussion

Spatiotemporal *Hes7* expression pattern is very unique, whereby it is restricted to the PSM and propagates (oscillates) from the posterior-end to the anterior-end of the PSM with 2-h periodicity in mice. In this study, we identified a narrow region within -1.5 to -1.1 kb from TSS in mouse *Hes7*, referred to as the C region in this study, that directs the specific expression of reporter gene in the PSM during mouse embryogenesis. At the molecular level, we found E-boxes, T-boxes, and RBPj-binding sites in the C region and further demonstrated that these elements are crucial for the restricted expression of the reporter gene in the PSM. Furthermore, this study raises the possibility

that the Notch signaling pathway, the transcriptional activators, *Msn1* and *Tbx6*, and the transcriptional repressors, *Tbx18*, *Ripply1/2*, and *Hes7*, participate as novel factors for the C region's activation/repression.

Our study using transgenic founder assays revealed that this C region, which is highly conserved among several species, is sufficient to direct expression of the reporter gene in the PSM specifically during mouse embryogenesis (Figs 1 and 2). Our current study further dissected the molecular mechanisms for PSM-specific *Hes7* expression. *In situ* hybridization for *lacZ* mRNA (Fig. 2B) showed that only two of 16 embryos with mutated E-box demonstrated positive, but obscure, signals. In addition, luciferase assays (Fig. 3H) demonstrated that the mutated E-box was completely unresponsive to the activation by *Tbx6/Msn1/NICD*. These findings suggest that the mutated E-box has no potential to activate gene expression in the PSM. In contrast to the mutated E-box, the mutated T-box had produced *lacZ* signals in six of eight embryos (Fig. 2B) and had increased the luciferase activity by *Tbx6/Msn1/NICD* (Fig. 3H), although the activity was much lower than that of WT C region. We therefore conclude that E-boxes and T-boxes, including the RBPj-binding site, are critical and auxiliary, respectively. Moreover, X-gal staining and *in situ* hybridization for Deletion1 or -2 (Fig. 1, I–L, and Fig. S2) suggest that E-box1–3 and T-box1/2 are functional, because these results showed no/weak signals at the posterior-end PSM. The reason no/weak signals were restricted at the posterior-end PSM could be that the gene expression driven by the C region without any of these elements is very weak and under detectable levels by X-gal staining and *in situ* hybridization at the posterior-end PSM; however, after a while, reporter mRNA and protein slowly accumulated to reach detectable levels.

It has been reported that the somite formation does not take place when *Msn1* or *Tbx6* is knocked out in mice (12, 20, 21). In addition to *Msn1* and *Tbx6*, somite formation does not occur properly when *Hes7* is deficient (6). Moreover, *Msn1* or components of the Notch pathway knockout mice express less *Hes7* in the PSM (10, 22, 23). These reports strongly support our findings that *Msn1*, *Tbx6*, and Notch pathway are upstream of *Hes7*. Furthermore, we raise the possibility that the combination of *Msn1*, Notch signaling, and *Tbx6* induces *Hes7* expression via the C region in the mouse PSM. Interestingly, synergistic transcriptional activation by *Tbx6* with other transcriptional factors during somitogenesis has been reported; for example, *Tbx6* cooperates with Wnt signaling for *Dll1* and *Msn1* induction (24, 25) and with Notch signaling for *Mesp2* induction in mouse (26). In *Xenopus*, *Tbx6* activates *bowline*, a *Xenopus Ripply* homologue, in synergy with bHLH transcription factors, *Thylacine1* and *E47* (27). Moreover, we also raise the possibility that T-box1–3 elements are essential to form the optimal three-dimensional structure of the C region with *Tbx6/Msn1/NICD* for the synergistic activation. Although further investigations will be required to address whether and how *Tbx6/Msn1/NICD* form a complex with the C region for the complete *Hes7* activation, our finding nonetheless had shed light on a new role of *Tbx6* in somitogenesis.

Our findings in this study also raised the possibility that T-box elements function to repress *Hes7* expression in the

anterior-most PSM (S-I and S0) and somites by binding with *Tbx18*. This dual function of T-boxes could be one of the mechanisms for the termination and inhibition of *Hes7* expression at the anterior-most PSM and somites, respectively. Another key factor for *Hes7* repression is *Ripply1/2*. *Ripply1/2* have already been shown to repress *Tbx6* expression by two different ways. One is the conversion of *Xenopus* and zebrafish *Tbx6* from transcriptional activator to suppressor by binding with Groucho/TLE co-repressors (18, 19). The other is the elimination of *Tbx6* protein by unknown mechanisms (28). In this study, we demonstrated that mouse *Ripply1/2* could bind with mouse *Tbx6* and repress the expression of *Hes7 in vitro* (Fig. 4, B and C). Our data suggest that, at the anterior-most PSM in mouse, *Ripply* suppresses *Hes7* expression through recruitment to T-box elements with *Tbx6/Groucho/TLE* co-repressors and/or by eliminating *Tbx6* protein (Fig. 5). However, because *Hes7* expression patterns are normal even in *Ripply1* and -2 double knockout embryos (28), the *Hes7* termination mechanism by *Ripply1/2* might be ancillary and that by *Tbx18* is primary. It is noteworthy that an interesting paper has reported that *Mesp2*, which expresses S-I, suppresses Notch signaling via destabilizing Mastermind-like 1, a coactivator of Notch signaling (29). The suppression of Notch signaling by *Mesp2* at the anterior-most PSM shown in that report could be another potential mechanism for the termination of *Hes7* expression. Taking their findings and our current analyses together, we establish that to spatiotemporally express and terminate *Hes7* expression at the PSM, a web of transcriptional mechanisms is required during somitogenesis and that the *Hes7* suppressor element would be important for a proper maintenance of the functional *Hes7* domain as well as activator elements.

González *et al.* (30) reported that *Hes7* expression is controlled by *Tbx6* and Wnt signaling. They have identified an essential 400-bp region (–1.4 to –1.0 kbp from TSS) for proper *Hes7* expression, which is almost identical to our *Hes7* essential region (–1.5 to –1.1 kbp from TSS). Furthermore, they have also found that the activity of the *Hes7* promoter in mouse PSM requires *Tbx6*-binding sites within this 400-bp region. These findings support our current study, although their distal T-box corresponds to T-box2 in our study, and the proximal one, which we missed as T-box, overlaps with E-box3 identified in our study. Intriguingly, they have mentioned that downstream molecules of the Wnt pathway activate the *Hes7* promoter cooperatively with *Tbx6* in cell culture and are necessary for its proper expression in the mouse PSM. More interestingly, they have shown that the expression of *Msn1*, one of the Wnt target genes and the activator for the *Hes7* essential region revealed in our study, is activated in embryos treated with LiCl, the inhibitor of GSK3 β , in which Wnt signaling is activated. Taken together, their study strongly supports our results that *Msn1* is associated with the activation of *Hes7* expression with *Tbx6*.

Our current findings demonstrated that the C region, including the specific elements of the C region, is sufficient for the restricted reporter mRNA expression in the PSM, and the C region is activated by a synergistic effect of *Msn1*, *Tbx6*, and Notch signaling and repressed by *Tbx18*, *Ripply2*, and *Hes7* in cell culture. However, we have not addressed whether the C

Promoter elements for restricted expression of *Hes7*

region and the regulatory factors are indispensable for the endogenous *Hes7* expression in the PSM. In addition, we cannot rule out the possibility that other existing shadow or cryptic enhancers such as long range (1 Mb or more) enhancer (31) and enhancer residing in introns (32) or in 3' downstream (33) may also be essential to *Hes7* expression. To uncover whether the C region, and which elements in the C region, are indispensable for the PSM-specific endogenous *Hes7* expression, further *in vivo* transcriptional analyses of the endogenous *Hes7* promoter deleting the whole C region or knocking-in the C region with mutated elements will be required. As mentioned above, previous reports suggest that *Msgn1* and Notch pathway are upstream of *Hes7*; however, detailed analyses of endogenous *Hes7* expression in gene-modified mice in which the expression levels of *Msgn1*, *Tbx6*, components of Notch signaling, *Tbx18*, or *Ripply2* are altered will be required.

Finally, although we demonstrated that (i) C region has multiple E-boxes, (ii) the bHLH-type activator *Msgn1* and the repressor *Hes7* occupy E-box1 and E-box2 and -3, respectively (Figs. 3D and 4E), and (iii) *Hes7* can repress *Msgn1*/*Tbx6*/NICD-dependent activation (Fig. 4D). Although we were unable to demonstrate the oscillation by the 5.3-kb fragment (Fig. 1R), we were unable to evince that the C region is enough for *Hes7* oscillation, in that we could not detect the oscillatory *lacZ* mRNA expression pattern driven by the C region (Fig. 1T). As it has been known that multiple enhancers act on gene expression to ensure robustness (34), multiple additional elements, such as E/N-boxes near the transcription start site as reported previously (35), might be needed for *Hes7* to achieve and maintain oscillatory expression. Further analysis therefore will be required to find a minimum set of oscillatory elements for establishment of *Hes7* oscillatory expression.

Experimental procedures

Animals

CD1 mice used in this study were purchased from SLC (Japan). Our experiments with mice have been approved by The Animal Care Committee of Nara Institute of Science and Technology (NAIST). These experiments were conducted in accordance with guidelines that were established by the Science Council of Japan.

Reporter constructs and transgenic mice

Hes7 upstream region was cloned by conventional molecular biological methods. Upstream fragment was PCR-amplified and inserted into pBluescriptII (Stratagene) with *lacZ* gene and *SV40* poly(A) signal. Human β -globin minimal promoter, being synthesized as a double-stranded oligonucleotide, was inserted into a reporter vector for the enhancer assay. Sequences for human β -globin minimal promoter were as follows: Fw, TCC CGG GCT GGG CAT AAA AGT CAG GGC AGA GCC ATC TAT TGC TTA CAT TTG CTT C, and Rv, GAA GCA AAT GTA AGC AAT AGA TGG CTC TGC CCT GAC TTT TAT GCC CAG CCC GGG A. To make transgenic mice, the constructs were linearized and injected into fertilized eggs from CD1 mice by the animal facility of NAIST.

X-gal staining and *in situ* hybridization

Transgenic mice were dissected and analyzed at embryonic day 10.5 (E10.5). For X-gal staining, embryos were fixed in 0.5% glutaraldehyde with 2 mM $MgCl_2$ at 4 °C for 30 min. Then, these embryos were soaked in color solution (1 mg/ml 5-bromo-4-chloro-3-indolyl- β -D-galactoside, 5 mM potassium ferricyanide, 5 mM potassium ferrocyanide, 2 mM $MgCl_2$, Nonidet P-40, 0.01% sodium deoxycholate) at 37 °C overnight. Whole-mount *in situ* hybridization of mouse embryos was performed as described previously (5).

Luciferase assay

Hes7 C region followed by human β -globin minimal promoter were inserted into pGL3-Basic vector (Promega). Transcription factors were cloned by PCR with cDNA from mouse PSM. 5'-UTR and the coding region of each gene were inserted into pcDNA3 (Invitrogen), including FLAG, HA, or Myc tag at the 3'-end. 3×10^4 NIH3T3 cells were plated in each well of a 24-well plate and were cultured in 10% fetal bovine serum/Dulbecco's modified Eagle's medium at 5% CO_2 . After 24 h, cells were co-transfected with 300 ng of *Hes7* reporter and 200 ng of expression vector of transcription factors using TransIT LT1 (Mirus). Transfected cells were lysed after 24 h of culture, and reporter activity was measured using a Dual-Luciferase assay system (Promega) and analyzed by ARBO (PerkinElmer Life Sciences). Firefly luciferase activity of the reporter was normalized by the activity of *Renilla* luciferase under control of SV40 promoter.

Mutagenesis

Site-directed mutagenesis was performed as described previously (36). Sequences were substituted as follows: T-box1, AGG TGT GGG AA to AGG TtT taa Ac; T-box2, CCA CAC CC to CgA tAt CC; T-box3, CCA CAC AT to CgA tAt AT; E-box1, CAT ATG to gtT Aac; E-box2, CAC GTG to gtC Gac; E-box3, CAG GTG to gtG Gac; E-box4, CAT CTG to gtT Cac; E-box5, CAT TTG to gtT Tac; and E-box6, CAA ATG to gtA Aac. Small letters indicate mutated nucleotides.

In silico promoter analysis

A homology between human *Hes7* upstream and mouse *Hes7* upstream was analyzed by VISTA (37, 38). To predict T-boxes, E-boxes, or RBPj-binding sites in the C region, YMACACY or complementary, CANNTG, or YRTGDGAD or complementary were referred to as T-box, E-box, or RBPj-binding site, respectively (5, 21, 39). Homology search among C regions of *H. sapiens*, *P. abelii*, *B. taurus*, and *M. musculus* was performed by ClustalW version 2.1.

Oligo-DNA pulldown assay

COS7 cells were seeded in 10-cm dish (4×10^5 cells/dish), transfected with 15 μ g of expression vectors, and cultured for 48 h. Cells were lysed in binding buffer (10 mM Tris, pH 8.0, 150 mM NaCl, 1 mM $MgCl_2$, 0.5% Nonidet P-40, 5% glycerol) with protease inhibitor mixture (Nacalai Tesque, Japan). After removing debris by centrifugation, 30 μ l of 50% slurry streptavidin-Sepharose beads (GE Healthcare) and 200 pmol of dou-

ble-stranded oligonucleotide conjugated with biotin at each 5'-end were added to the cell lysates. The mixture was incubated at 4 °C for 30 min with rotation. Sepharose beads were washed with the binding buffer three times. Then, the resultant pulldown samples were separated by SDS-PAGE on precast 5–20% polyacrylamide gels (Nacalai Tesque, Japan). Proteins were then transferred to PVDF membranes using a wet electroblotting apparatus. The membranes were blocked using 5% skim milk in TBS with 0.1% Tween (TBS-T) for 1 h and incubated with anti-Myc (monoclonal, PL14, MBL, Japan) overnight, followed by incubation with anti-mouse IgG conjugated with horseradish peroxidase (GE Healthcare). Signals were visualized by the enhanced chemiluminescence detection system according to the manufacturer's instruction (Nacalai Tesque, Japan). Oligo-DNA sequences are as follows: E-box1 FW, 5'-AAA GTC ATT CCA TAT GGC CAG GGG CG-3', and E-box1 RV, 5'-CGC CCC TGG CCA TAT GGA ATG ACT TT-3'; E-box1 mut FW, 5'-AAA GTC ATT Cgc TAG GGC CAG GGG CG-3', and E-box1 mut RV, 5'-CGC CCC TGG CCc TAG cGA ATG ACT TT-3'; E-box2 and -3 FW, 5'-CCC CGA GCC TCA CGT GCA GGT GAG AAA AAC TC-3', and E-box2 and -3 RV, 5'-GAG TTT TTC TCA CCT GCA CGT GAG GCT CGG GG-3'; T-box1 FW, 5'-ACT TCT AGG TGT GGG AAA AGG TTG TAG-3', and T-box1 RV, 5'-CTA CAA CCT TTT CCC ACA CCT AGA AGT-3'; T-box1 mut FW, 5'-ACT TCT AGG TtT taa AcA AGG TTG TAG-3', and T-box1 mut RV, 5'-CTA CAA CCT TgT tta AaA CCT AGA AGT-3'. Small letters indicate mutated nucleotides.

ChIP assay

Mouse embryos (more than 120 embryos) were dissected at E10.5, and PSMs were collected in ice-cold PBS with protease inhibitor mixture. PSMs were dispersed by 0.05 w/v % trypsin/EDTA treatment for 3 min. Cells were fixed with 1% formaldehyde in PBS for 10 min at room temperature, and the fixation was stopped by adding 0.1 amount of 1.5 M glycine. After a brief centrifugation, cells were lysed with 200 ml of SDS lysis buffer (50 mM Tris-HCl, pH 8.0, 10 mM EDTA, 1% SDS). Cell lysates were sonicated genome using a bioruptor (Cosmo Bio) with power set at high and a 30-s on and 60-s off interval. After centrifugation to remove the insoluble fraction, supernatants were diluted with nine times the amount of dilution buffer (50 mM Tris-HCl, pH 8.0, 167 mM NaCl, 1.1% Triton X-100, 0.11% sodium deoxycholate), including protease inhibitor mixture. For pre-cleaning, samples were added 20 μ l of 50% slurry protein A-Sepharose (Nacalai Tesque, Japan) and incubated more than 4 h at 4 °C, followed by centrifugation to remove protein A-Sepharose. Tbx6 antibody (29) or Hes7 antiserum (35) were added to the pre-cleaned sample, respectively, and were incubated overnight at 4 °C. The sample was added with 20 μ l of 50% slurry protein A-Sepharose and incubated for more than 3 h at 4 °C. Resultant immunoprecipitated samples were washed with a series of buffers (RIPA buffer 1: 50 mM Tris-HCl, pH 8.0, 150 mM NaCl, 1 mM EDTA, 1% Triton X-100, 0.1% SDS, 0.1% sodium deoxycholate; RIPA buffer 2: 50 mM Tris-HCl, pH 8.0, 500 mM NaCl, 1 mM EDTA, 1% Triton X-100, 0.1% SDS, 0.1% sodium deoxycholate; LiCl buffer: 10 mM Tris-HCl, pH 8.0, 0.25 M LiCl, 1 mM EDTA, 0.5% Nonidet P-40, 0.5% sodium

deoxycholate; TE buffer: 10 mM Tris-HCl, pH 8.0, 1 mM EDTA, two times). For decross-linking and elution, elution buffer (10 mM Tris-HCl, pH 8.0, 300 mM NaCl, 5 mM EDTA, 0.5% SDS) was added to samples and incubated at 65 °C for 4 h. After decross-linking, DNA were purified and subjected to PCR amplification. The sequences of the forward and reverse primers are as follows: *Hes7* C ChIP FW: 5'-ATG TGA ACT TCT CAG AGG CAG ATC CAA TCC-3', and *Hes7* C ChIP RV: 5'-CCT TCC CAG AGG CCC TCC ACA TCC TG-3'.

Immunoprecipitation

HEK293T cells were seeded at 4×10^5 cells in a 10-cm dish, cultured for 24 h, and transfected with 5 μ g of each expression vectors or empty pcDNA3 vector. After 48 h of culture, cells were lysed in ice-cold TNE buffer (20 mM Tris-HCl, pH 8.0, 1 mM EDTA, pH 8.0, 1% Nonidet P-40, 150 mM NaCl) with protease inhibitor mixture. After removing debris by centrifugation, supernatants were incubated with 15 μ l of 50% slurry anti-FLAG M2-agarose (Sigma) overnight at 4 °C with rotation. The next day, agarose beads were washed three times with ice-cold TNE buffer, and resultant immunoprecipitated samples were separated by SDS-PAGE on precast 5–20% polyacrylamide gels (Nacalai Tesque, Japan). Proteins were then transferred to PVDF membranes using a wet electroblotting apparatus. The membranes were blocked using 5% skim milk in TBS-T for 1 h and incubated with anti-Myc or anti-FLAG (monoclonal, FLA-1, MBL, Japan) overnight, followed by incubation with anti-mouse IgG conjugated with horseradish peroxidase. Signals were visualized by the enhanced chemiluminescence detection system according to the manufacturer's instruction.

Author contributions—S. H., Y. N., T. M., and Y. B. data curation; S. H. formal analysis; S. H. and Y. N. investigation; S. H. and Y. N. writing-original draft; Y. N., T. M., and Y. B. conceptualization; Y. N. and Y. B. supervision; Y. N. and Y. B. project administration; Y. N. and Y. B. writing-review and editing; K. K. resources; Y. N. and Y. B. funding acquisition.

Acknowledgments—We thank Drs. Y. Yasuhiko and M. Saito for providing anti-Tbx6 antibody and for the generation of transgenic mice, respectively. We also thank R. Ahmed and Dr. F. D. Khaidizar for providing critical comments on the manuscript.

References

1. Saijoh, Y., Adachi, H., Mochida, K., Ohishi, S., Hirao, A., and Hamada, H. (1999) Distinct transcriptional regulatory mechanisms underlie left-right asymmetric expression of *lefty-1* and *lefty-2*. *Genes Dev.* **13**, 259–269 [CrossRef Medline](#)
2. Meno, C., Shimono, A., Saijoh, Y., Yashiro, K., Mochida, K., Ohishi, S., Noji, S., Kondoh, H., and Hamada, H. (1998) *Lefty-1* is required for left-right determination as a regulator of *lefty-2* and *nodal*. *Cell* **94**, 287–297 [CrossRef Medline](#)
3. Meno, C., Gritsman, K., Ohishi, S., Ohfuji, Y., Heckscher, E., Mochida, K., Shimono, A., Kondoh, H., Talbot, W. S., Robertson, E. J., Schier, A. F., and Hamada, H. (1999) Mouse *lefty2* and zebrafish *antivin* are feedback inhibitors of *nodal* signaling during vertebrate gastrulation. *Mol. Cell* **4**, 287–298 [CrossRef Medline](#)
4. Meno, C., Takeuchi, J., Sakuma, R., Koshiba-Takeuchi, K., Ohishi, S., Saijoh, Y., Miyazaki, J., ten Dijke, P., Ogura, T., and Hamada, H. (2001) Diffusion of *nodal* signaling activity in the absence of the feedback inhibitor *lefty2*. *Dev. Cell* **1**, 127–138 [CrossRef Medline](#)

Promoter elements for restricted expression of *Hes7*

- Bessho, Y., Miyoshi, G., Sakata, R., and Kageyama, R. (2001) *Hes7*: a bHLH-type repressor gene regulated by Notch and expressed in the presomitic mesoderm. *Genes Cells* **6**, 175–185 [CrossRef Medline](#)
- Bessho, Y., Sakata, R., Komatsu, S., Shiota, K., Yamada, S., and Kageyama, R. (2001) Dynamic expression and essential functions of *Hes7* in somite segmentation. *Genes Dev.* **15**, 2642–2647 [CrossRef Medline](#)
- Kageyama, R., Ohtsuka, T., and Kobayashi, T. (2007) The *Hes* gene family: repressors and oscillators that orchestrate embryogenesis. *Development* **134**, 1243–1251 [CrossRef Medline](#)
- Dequéant, M. L., and Pourquié, O. (2008) Segmental patterning of the vertebrate embryonic axis. *Nat. Rev. Genet.* **9**, 370–382 [CrossRef Medline](#)
- Pourquié, O. (2011) Vertebrate segmentation: from cyclic gene networks to scoliosis. *Cell* **145**, 650–663 [CrossRef Medline](#)
- Niwa, Y., Masamizu, Y., Liu, T., Nakayama, R., Deng, C. X., and Kageyama, R. (2007) The initiation and propagation of *Hes7* oscillation are cooperatively regulated by Fgf and notch signaling in the somite segmentation clock. *Dev. Cell* **13**, 298–304 [CrossRef Medline](#)
- Hayashi, S., Shimoda, T., Nakajima, M., Tsukada, Y., Sakumura, Y., Dale, J. K., Maroto, M., Kohno, K., Matsui, T., and Bessho, Y. (2009) *Sprout4*, an FGF inhibitor, displays cyclic gene expression under the control of the notch segmentation clock in the mouse PSM. *PLoS One* **4**, e5603 [CrossRef Medline](#)
- Yoon, J. K., Moon, R. T., and Wold, B. (2000) The bHLH class protein pMesogenin1 can specify paraxial mesoderm phenotypes. *Dev. Biol.* **222**, 376–391 [CrossRef Medline](#)
- Wardle, F. C., and Papaioannou, V. E. (2008) Teasing out T-box targets in early mesoderm. *Curr. Opin. Genet. Dev.* **18**, 418–425 [CrossRef Medline](#)
- Chapman, D. L., Agulnik, I., Hancock, S., Silver, L. M., and Papaioannou, V. E. (1996) *Tbx6*, a mouse T-box gene implicated in paraxial mesoderm formation at gastrulation. *Dev. Biol.* **180**, 534–542 [CrossRef Medline](#)
- Barrantes, I. B., Elia, A. J., Wunsch, K., Hrabe de Angelis, M. H., Mak, T. W., Rossant, J., Conlon, R. A., Gossler, A., and de la Pompa, J. L. (1999) Interaction between Notch signalling and Lunatic fringe during somite boundary formation in the mouse. *Curr. Biol.* **9**, 470–480 [CrossRef Medline](#)
- Kraus, F., Haenig, B., and Kispert, A. (2001) Cloning and expression analysis of the mouse T-box gene *Tbx18*. *Mech. Dev.* **100**, 83–86 [CrossRef Medline](#)
- Biris, K. K., Dunty, W. C., Jr, and Yamaguchi, T. P. (2007) Mouse *Ripply2* is downstream of *Wnt3a* and is dynamically expressed during somitogenesis. *Dev. Dyn.* **236**, 3167–3172 [CrossRef Medline](#)
- Kawamura, A., Koshida, S., and Takada, S. (2008) Activator-to-repressor conversion of T-box transcription factors by the Ripply family of Groucho/TLE-associated mediators. *Mol. Cell. Biol.* **28**, 3236–3244 [CrossRef Medline](#)
- Kondow, A., Hitachi, K., Okabayashi, K., Hayashi, N., and Asashima, M. (2007) Bowline mediates association of the transcriptional co-repressor XGrg-4 with *Tbx6* during somitogenesis in *Xenopus*. *Biochem. Biophys. Res. Commun.* **359**, 959–964 [CrossRef Medline](#)
- Chapman, D. L., and Papaioannou, V. E. (1998) Three neural tubes in mouse embryos with mutations in the T-box gene *Tbx6*. *Nature* **391**, 695–697 [CrossRef Medline](#)
- Nikaido, M., Kawakami, A., Sawada, A., Furutani-Seiki, M., Takeda, H., and Araki, K. (2002) *Tbx24*, encoding a T-box protein, is mutated in the zebrafish somite-segmentation mutant fused somites. *Nat. Genet.* **31**, 195–199 [CrossRef Medline](#)
- Ferjentsik, Z., Hayashi, S., Dale, J. K., Bessho, Y., Herreman, A., De Strooper, B., del Monte, G., de la Pompa, J. L., and Maroto, M. (2009) Notch is a critical component of the mouse somitogenesis oscillator and is essential for the formation of the somites. *PLoS Genet.* **5**, e1000662 [CrossRef Medline](#)
- Chalamalasetty, R. B., Dunty, W. C., Jr, Biris, K. K., Ajima, R., Iacovino, M., Beisaw, A., Feigenbaum, L., Chapman, D. L., Yoon, J. K., Kyba, M., and Yamaguchi, T. P. (2011) The *Wnt3a/β-catenin* target gene *Mesogenin1* controls the segmentation clock by activating a Notch signalling program. *Nat. Commun.* **2**, 390 [CrossRef Medline](#)
- Hofmann, M., Schuster-Gossler, K., Watabe-Rudolph, M., Aulehla, A., Herrmann, B. G., and Gossler, A. (2004) WNT signaling, in synergy with T/TBX6, controls Notch signaling by regulating *Dll1* expression in the presomitic mesoderm of mouse embryos. *Genes Dev.* **18**, 2712–2717 [CrossRef Medline](#)
- Wittler, L., Shin, E. H., Grote, P., Kispert, A., Beckers, A., Gossler, A., Werber, M., and Herrmann, B. G. (2007) Expression of *Mesg1* in the presomitic mesoderm is controlled by synergism of WNT signalling and *Tbx6*. *EMBO Rep.* **8**, 784–789 [CrossRef Medline](#)
- Yasuhiko, Y., Kitajima, S., Takahashi, Y., Oginuma, M., Kagiwada, H., Kanno, J., and Saga, Y. (2008) Functional importance of evolutionally conserved *Tbx6* binding sites in the presomitic mesoderm-specific enhancer of *Mesp2*. *Development* **135**, 3511–3519 [CrossRef Medline](#)
- Hitachi, K., Kondow, A., Danno, H., Inui, M., Uchiyama, H., and Asashima, M. (2008) *Tbx6*, *Thylacine1*, and *E47* synergistically activate bowline expression in *Xenopus* somitogenesis. *Dev. Biol.* **313**, 816–828 [CrossRef Medline](#)
- Takahashi, J., Ohbayashi, A., Oginuma, M., Saito, D., Mochizuki, A., Saga, Y., and Takada, S. (2010) Analysis of *Ripply1/2*-deficient mouse embryos reveals a mechanism underlying the rostro-caudal patterning within a somite. *Dev. Biol.* **342**, 134–145 [CrossRef Medline](#)
- Sasaki, N., Kiso, M., Kitagawa, M., and Saga, Y. (2011) The repression of Notch signaling occurs via the destabilization of mastermind-like 1 by *Mesp2* and is essential for somitogenesis. *Development* **138**, 55–64 [CrossRef Medline](#)
- González, A., Manosalva, I., Liu, T., and Kageyama, R. (2013) Control of *Hes7* expression by *Tbx6*, the Wnt pathway and the chemical Gsk3 inhibitor LiCl in the mouse segmentation clock. *PLoS One* **8**, e53323 [CrossRef Medline](#)
- Kleinjan, D. A., and van Heyningen, V. (2005) Long-range control of gene expression: emerging mechanisms and disruption in disease. *Am. J. Hum. Genet.* **76**, 8–32 [CrossRef Medline](#)
- Garnett, A. T., Han, T. M., Gilchrist, M. J., Smith, J. C., Eisen, M. B., Wardle, F. C., and Amacher, S. L. (2009) Identification of direct T-box target genes in the developing zebrafish mesoderm. *Development* **136**, 749–760 [CrossRef Medline](#)
- Lieven, O., Knobloch, J., and Rütger, U. (2010) The regulation of *Dkk1* expression during embryonic development. *Dev. Biol.* **340**, 256–268 [CrossRef Medline](#)
- Frankel, N., Davis, G. K., Vargas, D., Wang, S., Payre, F., and Stern, D. L. (2010) Phenotypic robustness conferred by apparently redundant transcriptional enhancers. *Nature* **466**, 490–493 [CrossRef Medline](#)
- Bessho, Y., Hirata, H., Masamizu, Y., and Kageyama, R. (2003) Periodic repression by the bHLH factor *Hes7* is an essential mechanism for the somite segmentation clock. *Genes Dev.* **17**, 1451–1456 [CrossRef Medline](#)
- Sawano, A., and Miyawaki, A. (2000) Directed evolution of green fluorescent protein by a new versatile PCR strategy for site-directed and semi-random mutagenesis. *Nucleic Acids Res.* **28**, E78 [CrossRef Medline](#)
- Mayor, C., Brudno, M., Schwartz, J. R., Poliakov, A., Rubin, E. M., Frazer, K. A., Pachter, L. S., and Dubchak, I. (2000) VISTA: visualizing global DNA sequence alignments of arbitrary length. *Bioinformatics* **16**, 1046–1047 [CrossRef Medline](#)
- Frazer, K. A., Pachter, L., Poliakov, A., Rubin, E. M., and Dubchak, I. (2004) VISTA: computational tools for comparative genomics. *Nucleic Acids Res.* **32**, W273–W279 [CrossRef Medline](#)
- Yasuhiko, Y., Haraguchi, S., Kitajima, S., Takahashi, Y., Kanno, J., and Saga, Y. (2006) *Tbx6*-mediated Notch signaling controls somite-specific *Mesp2* expression. *Proc. Natl. Acad. Sci. U.S.A.* **103**, 3651–3656 [CrossRef Medline](#)